Published in final edited form as:
Bone. 2008 April ; 42(4): 681–694. doi:10.1016/j.bone.2007.12.215.

Role of Genetic Background in Determining Phenotypic Severity Throughout Postnatal Development and at Peak Bone Mass in *Col1a2* Deficient Mice (*oim*)

Stephanie M. Carleton[1,2], **Daniel J. McBride**[3], **William L. Carson**[4], **Carolyn E. Huntington**[5], **Kristin L. Twenter**[2], **Kristin M. Rolwes**[2], **Christopher T. Winkelmann**[6], **J. Steve Morris**[5], **Jeremy F. Taylor**[7], and **Charlotte L. Phillips**[1,2,8]

1*Genetics Area Program, University of Missouri-Columbia, Columbia, Missouri, 65212.*

2*Department of Biochemistry, University of Missouri-Columbia, Columbia, Missouri, 65212.*

3*Division of Endocrinology, Diabetes and Nutrition, University of Maryland-Baltimore, Baltimore, MD, 21201.*

4*Comparative Orthopedic Laboratory, University of Missouri-Columbia, Columbia, Missouri, 65212.*

5*University of Missouri Research Reactor Center, University of Missouri-Columbia, Columbia, Missouri, 65212.*

6*Department of Veterinary Pathobiology, University of Missouri-Columbia, Columbia, Missouri, 65212.*

7*Department of Animal Sciences, University of Missouri-Columbia, Columbia, Missouri, 65212.*

8*Department of Child Health, University of Missouri-Columbia, Columbia, Missouri, 65212.*

Abstract

Osteogenesis imperfecta (OI) is a genetically and clinically heterogeneous disease characterized by extreme bone fragility. Although fracture numbers tend to decrease post-puberty, OI patients can exhibit significant variation in clinical outcome, even among related individuals harboring the same mutation. OI most frequently results from mutations in type I collagen genes, yet how genetic background impacts phenotypic outcome remains unclear. Therefore, we analyzed the phenotypic severity of a known proα2(I) collagen gene defect (*oim*) on two genetic backgrounds (congenic C57BL/6J and outbred B6C3Fe) throughout postnatal development to discern the phenotypic contributions of the *Col1a2* locus relative to the contribution of the genetic background.

To this end, femora and tibiae were isolated from wildtype (Wt) and homozygous (*oim/oim*) mice of each strain at 1, 2 and 4 months of age. Femoral geometry was determined via μCT prior to torsional loading to failure to assess bone structural and material biomechanical properties. Changes in mineral composition, collagen content and bone turnover were determined using neutron activation analyses, hydroxyproline content and serum pyridinoline crosslinks.

Corresponding Author: Charlotte L. Phillips, Ph.D., Associate Professor, Departments of Biochemistry and Child Health, University of Missouri-Columbia, 1 Hospital Dr., M743 Medical Sciences Bldg., Columbia, MO 65212, Phone: (573) 882-5122, Fax: (573) 884-4597, Email: PhillipsCL@missouri.edu.

μCT analysis demonstrated genotype-, strain- and age-associated changes in femoral geometry as well as a marked decrease in the amount of bone in *oim/oim* mice of both strains. *Oim/oim* mice of both strains, as well as C57BL/6J (B6) mice of all genotypes, had reduced femoral biomechanical strength properties compared to Wt at all ages, although they improved with age. Mineral levels of fluoride, magnesium and sodium were associated with biomechanical strength properties in both strains and all genotypes at all ages. *Oim/oim* animals also had reduced collagen content as compared to Wt at all ages. Serum pyridinoline crosslinks were highest at two months of age, regardless of strain or genotype.

Strain differences in bone parameters exist throughout development, implicating a role for genetic background in determining biomechanical strength. Age-associated improvements indicate that *oim/oim* animals partially compensate for their weaker bone material, but never attain Wt levels. These studies indicate the importance of genetic background in determining phenotypic severity, but the presence of the proα2(I) collagen gene defect and age of the animal are the primary determinants of phenotypic severity.

Keywords

Collagen; Osteogenesis Imperfecta; Biomechanics; Bone Mineralization; Rodent

INTRODUCTION

Osteogenesis imperfecta (OI) is a genetically and clinically heterogeneous disease commonly characterized by bone fragility. The genetic basis for OI is most commonly mutations in one of the two type I collagen genes, COL1A1 or COL1A2, that encode type I procollagen [1]. Type I collagen is normally found as a heterotrimer, made of two α1 chains and one α2 chain [$\alpha1(I)_2\alpha2(I)$], however a homotrimeric variant [$\alpha1(I)_3$] has also been identified embryonically [2,3], in some tumors [4–6] and may play a role during the wound healing process [7,8]. OI patients most often fall into one of the four Sillence classifications based on their clinical manifestations, with type III OI being the most severe form compatible with life [9]. These patients are generally wheelchair bound and have progressive bowing of the long bones, short stature, blue-gray sclera and reduced biomechanical integrity manifested by numerous fractures throughout life [1]. The osteogenesis imperfecta murine (*oim*) model exhibits an OI type III-like phenotype due to a single nucleotide deletion in the *Col1a2* gene leading to exclusion of the α2(I) chain from the type I collagen molecule, producing solely homotrimeric type I collagen [10]. This mouse model has been shown to have reduced biomechanical integrity in bones [11,12] and aorta [13], altered bone mineral composition [14] and reduced amounts of type I collagen in bones [12], aorta [13], tendon [15] and left ventricle [16].

More than 850 distinct OI-causing mutations have been identified to date [17,18]. These mutations are often limited to single individuals or families, thus complicating the study of genotype-phenotype correlations. With monogenetic disorders like OI, we anticipate that the mutations will be the primary determinants of phenotype; however, the presence of intra- and interfamilial variation suggests that genetic background and modifier genes also play a role in clinical severity. Differences in the contribution of genetic background to bone geometry and strength have been widely studied in inbred strains of mice, especially C57BL/6J (B6) and C3H/HeJ (C3) mice [19,20], and suggest that the decreased biomechanical properties in B6 mouse femurs are due in part to altered geometry and differences in bone turnover.

Although the skeletal fragility of the *oim* mouse model has been well studied, the impact of developmental stage on femoral geometry and biomechanical strength during postnatal development prior to three months of age has not been evaluated [11,12]. Prior to four months

of age the femur grows in both length and diameter, which impacts its geometry and biomechanical properties. Bones that are short or wide (all else being equal) are better able to withstand torsional loads and, therefore, will not break as easily as bones that are long or narrow [21]. During puberty, the porosity of the bone increases due to increased bone turnover, contributing to the increased number of fractures often seen in adolescents [21]. During pre-puberty and puberty, body and muscle mass increase, placing additional load on the bone. The mechanostat theory postulates that these added stresses act to improve the biomechanical properties of the bone, which responds to changes in loading with alterations in bone material and/or architecture [22]. Post-puberty, the rate of remodeling slows and porosity decreases, and the now larger bone continues to mineralize with a concomitant decrease in fracture rate [21]. This is consistent with observations that fracture number in OI patients tends to decrease post-puberty [23] and is also consistent with the theory that bones from OI patients play "catch-up" with increasing age in an attempt to correct for the reduction in the amount and quality of the bone [24].

The goal of this study was to evaluate the impact of genetic background on the *oim* mutation throughout postnatal mouse development. Femora and tibiae from wildtype (Wt), heterozygous (*oim*/+) and homozygous (*oim/oim*) animals of each of the two genetic backgrounds (the inbred C57BL/6J and the outbred B6C3Fe) were evaluated at 1, 2 and 4 months of age, corresponding to childhood, adolescence and post-puberty in humans [25] using a multi-tiered approach described in the materials and methods. To define the bone biomechanical integrity we measured the ability of the femoral diaphysis to resist torsional loading as determined by the torsional ultimate strength T_{max}, torsional stiffness K_s, and strain energy to failure U, which are a function of both the geometry (cross-section shape and size) and bone biomechanical material properties, as defined by tensile strength Su and shear modulus of elasticity G. Bone biomechanical material properties are in turn a function of the bone composition that can be further subdivided into contributions from the organic component (mainly type I collagen) and mineral component (primarily hydroxyapatite). We hypothesized that genetic background plays an important role in determining the severity of the *oim* phenotype at all ages. More specifically, we hypothesized that the *oim* clinical phenotype would be more severe when present on a mouse strain congenic for reduced, but phenotypically normal, bone mineral density such as C57BL/6J. We further hypothesized that the presence of the *oim* mutation would be the primary determinant of disease severity, regardless of age, with *oim/oim* animals remaining weaker than wildtype animals throughout development and that the severity of the disease will decrease post-puberty.

MATERIALS AND METHODS

Animals

Heterozygote B6C3Fe *a/a-Col1a2*$^{oim/J}$ (*oim*/+) animals were purchased from Jackson Laboratory (Bar Harbor, ME) and bred in an AAALAC accredited facility at the University of Missouri-Columbia to produce outbred Wt, outbred *oim*/+ and outbred *oim/oim* animals. The B6-*oim* line was produced by repeated backcrossing of *oim*/+ to wildtype C57BL/6J (B6) animals. The B6 background was verified to be >99% congenic after 11 generations by microsatellite analysis (RADIL, Columbia, MO). B6 *oim*/+ animals were then bred to produce the congenic B6 Wt, B6 *oim*/+ and B6 *oim/oim* animals. Animals had *ad libitum* access to food and water (Purina 5008 Formulab Diet; Purina Mills Inc., St Louis, MO). All experimental manipulations were performed under an approved University of Missouri Animal Care and Use Protocol. Genotypes (Wt, *oim*/+, *oim/oim*) of both strains were determined as previously described [14]. Animals of each genotype and strain were sacrificed at one, two and four months of age via CO_2 asphyxiation, weighed, blood harvested by exsanguination and serum isolated. Femurs and tibias were removed, cleaned of soft tissue attachments and snap frozen in liquid

nitrogen (tibias) or wrapped in strips of sterile gauze in sterile 1X phosphate buffered saline (femurs) for long-term storage at −80° C.

Experimental Strategy

Bone biomechanical integrity of femurs from two distinct mouse strains and three genotypes at three age points were analyzed using a multi-tiered approach. Torsional loading to failure was used to determine the diaphyseal structural properties torsional ultimate strength T_{max}, torsional stiffness Ks and energy to failure U. The combination of μCT analyses to evaluate femoral geometry and torsional loading to failure permitted separation of bone material properties shear modulus of elasticity G and tensile strength Su from diaphyseal structural properties. Bone material properties can be further subdivided into contributions from both the organic and mineral phases, which make up the two-component system of bone. The hydroxyproline assay was used to quantify type I collagen, the primary component of the organic phase, while neutron activation analysis was used to quantify calcium and phosphate as well as the individual trace elements found within the hydroxyapatite that makes up the mineral phase of bone.

μCT Analysis

Geometric parameters were defined from right femurs by microCT (μCT) scan analysis (MicroCAT II, Siemens Medical, Malvern, PA) prior to *ex vivo* torsional loading to failure. The μCT data acquisition scanning protocol was as follows: x-ray settings of 80kVp voltage and 400 microamp current with a 300 msec exposure. 360 projections were collected at one degree increments in a single rotation and calibration images were collected prior to data acquisition. The μCT image slices were reconstructed to give a cubic voxel dimension of 0.103 mm and analyzed using the Amira 3.1 software package (Mercury Computer Systems/TGS, Chelmsford, MA) to measure total femur length and locate the mid-shaft slice. The mid-shaft slice was modeled as a hollow elliptical cross-section with periosteal ($_p$) and endosteal ($_e$) anterior-posterior (d_p and d_e; minor diameters) and medio-lateral (D_p and D_e; major diameters) [12]. Their numerical values were determined by drawing a bone density histogram along the ellipse axes and reproducibly locating the edges of cortical bone defined as having a bone density threshold of $[P_{max} + (P_{max}-P_{min})/3]$. Marrow cavity diameter MCD is reported as the average of the two endosteal diameters. Cortical bone width CBW is reported as the average of the four thicknesses on the major and minor axes of the cortical mid-slice. Cortical polar moment of area type parameter [26] was calculated using $K = [\pi D_p^3 d_p^3 (1-q^4)/16(D_p^2+d_p^2)]$ where $q = D_e/D_p$. [per age/strain: Wt, n=8–18; *oim/oim*, n=8–14]

Torsional Loading to Failure

A steel cylindrical holder (Figure 1A) having two diametrically opposite side windows of length L with two remaining struts that held the ends aligned (protecting the fragile femur until testing) was machined for each femur to be tested. The femur's diaphyseal axis was held centered in the holder with two paper washers, one on each end of its exposed test section of length L while the ends were potted with 5 minute epoxy (Devcon, Danvers, MA). Using custom made pliers to hold the ends aligned, the holder struts were severed with a cut off wheel (Dremel, Racine, WI) followed by placing the holder in a test fixture (designed to apply a pure torsional load on the femur, Figure 1A) mounted on a TA-HDi testing machine (Stable Micro Systems, Surrey, UK). A cross bar prevented the proximal end of the holder-femur from rotating about its long axis while the distal end was rotated about its long axis at a constant speed of 0.75 rad/sec. The test machine's control software acquired the crosshead position, cable force F in grams, and sample time at a rate of 200 samples/sec. A digital camera was used to take pre- and post-test photos of each specimen (Figure 1B), as well as a video-audio clip of each test to obtain a record of the mode of femur failure. Applied torque T (Nmm) was

calculated using $T = [(F - F_{\text{friction in fixture}})*0.13006]$. T was plotted as a function of relative angular displacement θ (degrees) between the ends of the exposed section of femur shaft hereinafter called femur diaphysis or femur (Figure 2). Torsional stiffness Ks (Nmm/rad) of the femur's exposed test length L was determined as the slope of a line fit by linear regression to the initial linear region of this plot (between $5<T<10$ Nmm for 2 and 4 month samples; between $2<T<5$ for 1 month samples). Ultimate tensile strength Su (N/mm^2) of the femur's cortical bone was determined according to Roarck [26] by substituting the femur's torsional ultimate strength T_{max} and its mid-shaft cross section diameters into $Su = [16T_{max}/(\pi D_p d_p^2(1-q^4))]$. The shear modulus of elasticity G (N/mm^2) of the femur's cortical bone, was determined using $G = KsL/K$ according to Roarck [26] where the exposed length of femur was L=4.76 mm for one month (due to shorter femur) and 7 mm for two and four month femurs. The strain energy to failure absorbed in the femur U (Nmm), hereinafter abbreviated "energy to failure," was calculated as the work done by the testing machine on the femur-fixture assembly as the area under the T versus θ graph from T=2 to failure T_{max}. [per age/strain: Wt, n=8–12; *oim/oim*, n=6–12]

Trace Mineral Composition

Instrumental neutron activation analyses were performed to measure changes in trace mineral composition. Tibias were harvested and prepared according to Buff et al [27]. Standards and samples were activated by a thermal neutron flux of 5×10^{13} $n/cm^2/s$ (F, Na, Mg, Ca, K and Zn) or a 5×10^{12} $n/cm^2/s$ flux (P) for specific times (Table 1). A normalization factor was applied to the data from one month-old tibias to take into account different irradiation times between samples and standards to allow for quantitation using the standard comparator method as for two and four month-old tibias. Standards and samples were counted as previously described [27]. [per age: n=7–8 of each strain/genotype]

Hydroxyproline and Pyridinoline Content

Hydroxyproline, an amino acid unique to collagen, was quantified as a relative measure of collagen content [28]. Left femurs were lyophilized for three hours and then cut in half. Each half was weighed (Model AG245, Mettler Toledo, Columbus, OH) and measured. The proximal half was used for the determination of hydroxyproline content/mg bone as described by Stegemann and Stalder [29] [per age/strain: Wt, n=7–13; *oim*/+, n=8–10; *oim*, n=7–13]. Determination of serum pyridinoline, a marker of bone turnover, was done using the Metra Serum PYD EIA Kit according to the manufacturer's protocol (Quidel, San Diego, CA). Blood was stored with 5μl heparin on ice, centrifuged at 6000 rpm to separate serum from red blood cells and stored at −80° C. [per age/strain Wt, n=7–9; *oim/oim*, n=5–8]

Variance Component Estimation

Variance components were estimated using the fitting constants method for a mixed model in which the *Col1a2* genotype was fit as a random effect and age, gender and age × gender interaction terms were fit as fixed effects [30]. This method produces unbiased estimates of the genetic variance attributable to the *Col1a2* locus (V_L) and of the residual variance (V_E), which includes only environmental effects for the B6 mice, but environmental and residual polygenic effects for the outbred animals. The within strain variance for a trait was estimated as the sum of the terms $V_P=V_L + V_E$ and the percentage of the phenotypic variance attributable to the *Col1a2* locus was computed as $(100 \times V_L)/V_P$.

Statistical Analyses

All statistical analyses were performed using SAS (SAS Institute Inc., Cary, NC). Data from the three groups were analyzed as a $3 \times 2 \times 3$ factorial (3 genotypes, 2 strains, and 3 ages). When heterogeneous variations made it necessary, a log transformation was used to stabilize

heterogeneous variation. If this log transformation failed to stabilize the variation, a ranking procedure was used [31]. Mean differences were determined using Fisher's Least Significant Difference (LSD). Means and standard errors presented are untransformed values, although P values are for the transformed or ranked data. Relationships between bone biomechanics and bone mineral composition were determined using a simple linear regression analysis using SAS. All results are presented as mean ± standard error. Differences were considered to be statistically significant at a P value ≤ 0.05.

RESULTS

Geometric Properties

Oim/oim animals had reduced body mass as compared to Wt and *oim*/+ at all ages examined, regardless of mouse strain (Figure 3). B6 animals, regardless of genotype, also had reduced body mass as compared to outbred animals at all ages. Of the variation in total body mass, 45% and 36% was due to *Col1a2* genotype in B6 and outbred animals, respectively (Table 2). This difference was primarily due to difference in phenotypic variance between the strains; 7.5 g^2 in B6 and 13.4 g^2 in outbred animals, due to the presence of polygenic variance within the outbred animals. Femur length differed between the genotypes in a strain specific manner. Outbred *oim/oim* femurs were shorter than outbred Wt at all ages, while B6 *oim/oim* femurs were only significantly shorter than B6 Wt at four months of age ($p \leq 0.05$; Figure 4A). Outbred Wt femurs were longer than B6 Wt femurs at all ages, while outbred *oim/oim* had longer femurs than B6 *oim/oim* femurs at one and four months of age ($p \leq 0.05$). Femur length increased with age in both strains and in all genotypes ($p \leq 0.05$), except in outbred Wt animals, which had reached their maximum femur length by two months of age. Of the variation in femur length, 11% in B6 animals and 27% in outbred animals can be attributed to the *oim Col1a2* mutation, leaving 89% and 73% of the variation in femur length due to differences in genetic background (Table 2).

Differences in marrow cavity diameter MCD were seen in a genotype, strain and age dependent manner. Wt femurs of both strains had larger MCD than *oim/oim* femurs at four months of age ($p \leq 0.01$; Figure 4B). However, at one and two months of age, the only genotype differences were detected within the outbred strain, where Wt femurs had larger MCD than *oim/oim* femurs ($p \leq 0.0001$). Outbred Wt femurs had larger MCD than B6 Wt femurs at one month, but smaller MCD at four months of age ($p \leq 0.001$). B6 *oim/oim* femurs had larger MCD than outbred *oim/oim* femurs at two and four months of age ($p \leq 0.0001$). MCD also changed with age in a strain and genotype specific manner. Within the B6 strain, all genotypes increased their MCD between one and four months of age ($p \leq 0.0001$). Within the outbred strain, Wt animals had significant increases in MCD between one and two months of age, but a significant decrease between two and four months of age ($p \leq 0.01$). Of the variation in MCD, 24% and 52% was due to *Col1a2* genotype in B6 and outbred animals, respectively (Table 2). There were strain differences in both V_L (0.002 vs 0.009 mm^2) and V_p (0.008 vs 0.017 mm^2) between B6 and outbred mice, indicating that the polygenic component of variance within the outbred animals explained much less of the phenotypic variance than did *Col1a2* genotype.

Cortical bone width CBW was not significantly different between genotypes at any age (Figure 4C). B6 Wt femurs had smaller CBW than outbred Wt femurs at one month of age ($p \leq 0.02$). B6 *oim/oim* femurs had smaller CBW than outbred *oim/oim* femurs at four months of age ($p \leq 0.02$). Cortical bone width increased between one and four months of age in Wt and *oim/oim* mice of both strains ($p \leq 0.05$). Only 6 and 11% of the variation in CBW was due to *Col1a2* genotype in the B6 and outbred animals, respectively. However, the difference in V_E between the strains (0.0007 mm^2 and 0.0017 mm^2) is substantial and suggests that as much as 50% of the phenotypic variation within the outbred mice has a polygenic component (Table 2).

Oim/oim mice of both strains exhibited a significant reduction in the polar moment of area K compared to Wt mice of the same strain at all ages ($p \leq 0.01$; Figure 4D), indicating that *oim/oim* animals have less overall cortical bone cross section area distribution from its center (thus less resistance to applied torque all else being equal) than Wt animals. However, Wt and *oim/oim* mice of both strains showed age-associated increases between one and four months of age ($p \leq 0.0001$). Mouse strain differences in K were seen in a genotype- and age-specific manner. Outbred Wt femurs had a larger K at one month of age compared to B6 Wt ($p \leq 0.0001$) while B6 *oim/oim* femurs had a larger polar moment than outbred *oim/oim* femurs at two months of age ($p \leq 0.0003$). Genotype at the *Col1a2* locus explained 32% and 55% of the phenotypic variance in K in B6 and outbred animals (Table 2). The residual variances were similar among the strains [0.011 $(mm^4)^2$ vs 0.013 $(mm^4)^2$], indicating that variation in *Col1a2* is the primary genetic determinant of K and that there is very little polygenic involvement within the outbred mice. Although *oim*/+ mice of each strain exhibited greater variability, they typically produced mean values intermediate to Wt and *oim/oim* means for each of the parameters discussed above (data not shown).

Femoral Diaphyseal and Bone Material Properties

Genotype differences in diaphyseal torsional ultimate strength T_{max}, regardless of genetic background, were detected at each age point ($p \leq 0.0001$; Figure 5A). B6 and outbred *oim/oim* femurs exhibited T_{max} values which were 32% and 41%, 35% and 37%, and 48% and 44% of B6 and outbred Wt femurs at one, two and four months of age, respectively. Differences in T_{max} due to genetic background were only seen at one month in Wt and *oim*/+ (data not shown) femurs ($p \leq 0.01$), but not between *oim/oim* femurs of the two mouse strains. T_{max} increased with age in Wt and *oim/oim* femurs between one and four months of age ($p \leq 0.0001$), regardless of strain, although *oim/oim* femurs remained weaker than Wt at all ages. As with femoral geometry, *oim*/+ values were typically intermediate to Wt and *oim/oim* in both strains and at each age point for all biomechanical parameters (data not shown). Within the B6 and outbred strains, 52% and 67% of the variation in T_{max} can be attributed to *Col1a2* genotype, respectively (Table 2). There was little difference in V_E between the strains, suggesting a limited polygenic involvement in determining T_{max} within the outbred animals.

Cortical bone tensile strength Su also exhibited genotype differences at each age point, with the exception of one month old animals within the outbred strain, with *oim/oim* femurs having greatly reduced Su at all ages. However, unlike T_{max}, there appears to be a stronger genetic background component. Within the outbred strain, *oim/oim* Su was 73% and 61% of Wt Su at two and four months of age, respectively ($p \leq 0.01$; Figure 5B). Within the B6 strain, *oim/oim* Su was 50%, 43% and 62% of WT Su at one, two and four months of age, respectively ($p \leq 0.001$). Su also increased in all genotypes and in both strains with age ($p \leq 0.04$), although *oim/oim* remained weaker than Wt at all ages. The *Col1a2* locus explained 56% and 36% of the phenotypic variance in Su in B6 and outbred mice and the difference was primarily due to a large difference in V_E among the strains [55 $(N/mm^2)^2$ vs 126 $(N/mm^2)^2$], suggesting that as much as 36% of the phenotypic variance in Su within the outbred mice is due to polygenic background effects (Table 2).

Differences in diaphyseal torsional stiffness Ks, but not shear modulus of elasticity G of the bone material, due to genotype were seen between outbred Wt and *oim/oim* femurs at all ages ($p \leq 0.006$). B6 Wt and *oim/oim* femurs demonstrated genotype differences in Ks at two and four months ($p \leq 0.02$; Figure 5C). *Oim/oim* femurs also showed genetic background differences in G at two months of age ($p \leq 0.008$; Figure 5D). Ks and G both increased in all genotypes of both strains between one and four months ($p \leq 0001$). The *Col1a2* genotypes explained only 9% and 28% of the variation in Ks in B6 and outbred animals (Table 2). However, V_E was much greater within the outbred than the B6 animals [234 $(Nmm/radian)^2$ vs 146 $(Nmm/radian)^2$]

suggesting that there is no polygenic contribution to this parameter in the outbred mice. The *Col1a2* genotypes explained less than 5% of the variation in shear modulus of elasticity in both strains (Table 2). However, the difference in V_E between the B6 and outbred mice suggests that as much as 22% of the variance in shear modulus of elasticity in the outbred mice is polygenic (Table 2).

Genotype differences in diaphyseal energy to failure U were also seen at each age point, as *oim/oim* femurs were not able to absorb as much energy as Wt prior to fracturing (Figure 5E). B6 and outbred *oim/oim* femurs could absorb only 15% and 24%, and 23% and 28% of the energy prior to fracture of two and four month old Wt femurs of the same genetic background respectively ($p \leq 0.0001$). Mouse strain differences were seen in a genotype and age specific manner. Wt femurs showed strain differences at one and two months ($p \leq 0.05$) while *oim/oim* femurs only showed strain differences at four months of age ($p \leq 0.03$). The only age-associated changes in U were in outbred *oim/oim* and B6 Wt between one and four months of age ($p \leq 0.04$). Though U did increase with age in outbred Wt femurs, substantial intersample variation prevented the p value from reaching significance ($p = 0.1$). The *Col1a2* genotype explained 54 and 52% of the variance in energy to failure (Table 2); however, V_L and V_P were both approximately 2.5 fold greater among the outbred than among the B6 animals. This suggests the presence of modifier genes influencing this variable within these strains of mice.

The exposed femur length L for one month animals was 4.76 mm due to its short overall length, and 7mm for the two and four month animals. Theoretically torsional ultimate strength T_{max}, shear modulus of elasticity G and tensile strength Su are independent of length L. However, torsional stiffness Ks and energy to failure U are a function of L. To address this, the one month Ks and U results were normalized to 7 mm length equivalent values by using $Ks_7=(4.76/7)*(Ks_{4.76})$ and $U_7=(7/4.76)*(U_{4.76})$. Statistically, the normalized results produced the same statistical significance as non-normalized results.

Trace Mineral Composition

Trace mineral composition of *oim/oim* tibias was also altered as compared to Wt in both mouse strains in a mineral-specific and age-specific manner (Table 3). Increased levels of fluoride and magnesium are associated with reduced diaphyseal torsional ultimate strength T_{max} (Figure 6; Table 4) as well as strain energy to failure U and cortical bone tensile strength Su (data not shown as trends are similar to T_{max}). Conversely, increased levels of sodium are associated with increased T_{max}, U and Su (Figure 6; Table 4). Fluoride inversely associates with T_{max}, Su and U regardless of genetic background in an age-specific manner (representative graph for four month old animals shown in Figure 6A). Both *oim/oim* mouse strains had elevated levels of fluoride and magnesium as compared to their Wt littermates, with corresponding reduced strength parameters T_{max}, Su and U values, regardless of age (Table 3 and Table 4). Older animals within a strain-genotype group consistently had increased levels of fluoride with, however, increased strength parameters compared to their younger counterparts. *Oim/oim* tibias also had elevated levels of magnesium as compared to Wt tibias and this also corresponded to reductions in T_{max} (Table 3 and Table 4; Figure 6B) and Su and U (data not shown), but not in an age-specific manner. Sodium positively associated with T_{max} (Figure 6C; Table 4) and Su and U (data not shown), regardless of genetic background and age, with one exception being outbred animals at one month of age. Zinc also has significant interactions with Tmax, Su and U (Table 4). Phosphorus, calcium, potassium, and Ca/P ratios were also analyzed at each time point. These minerals exhibit strain-, genotype- and age-associated changes (Table 3), although the significance of these changes is unclear as these minerals did not have an association with femoral diaphyseal or bone strength properties (Table 4). Variation in specific minerals also has a genetic background component (Table 2). Approximately 70% of the variation in fluoride, sodium and magnesium within the B6 line was due to the *oim*

Col1a2 mutation, while only 41–56% of variation in the outbred line was due to the *oim* mutation. The variance due to *Col1a2*, V_L, on trace mineral composition was consistently larger in the B6 line than in the outbred mice, suggesting that epistatic modifier loci may significantly impact trace mineral acquisition.

Hydroxyproline and Pyridinoline Content

Oim/oim femurs contained less hydroxyproline/mg bone than did their Wt counterparts at all ages, regardless of genetic background ($p \leq 0.02$; Figure 7A). Differences in hydroxyproline content due to genetic background were only seen between four month-old Wt femurs with B6 femurs having more hydroxyproline than outbred Wt femurs ($p \leq 0.01$). Femurs from four month-old mice of all genotypes and in both strains had more hydroxyproline than their one-month counterparts ($p \leq 0.05$). Thirty seven percent of the variation in the amount of hydroxyproline in femora can be attributed to variation in *Col1a2* (Table 2). There was no indication of a polygenic contribution to this phenotype within the outbred mice.

Serum pyridinoline crosslinks demonstrated age, strain and genotype associated differences. B6 animals of all genotypes, as well as outbred wildtype animals, had significantly more pyridinoline crosslinks in their serum at two months of age than at one or four months of age ($p \leq 0.02$; Figure 7B). Outbred *oim*/+ animals had significant differences between one and four months of age ($p \leq 0.03$; data not shown) while outbred *oim/oim* animals did not have age-associated differences in serum pyridinoline content. Differences due to genetic background were only seen at four months of age in outbred *oim*/+ (data not shown) and *oim/oim* mice ($p \leq 0.007$). Genotype differences in serum pyridinoline content were only seen between outbred Wt and outbred *oim*/+ mice at two months of age ($p \leq 0.03$). The *Col1a2* locus explained little of the phenotypic variation (0.3 and 3%) in serum pyridinoline crosslinks in B6 and outbred mice and there was no evidence for an effect due to polygenes within the outbred animals (Table 2).

DISCUSSION

Our goal was to determine the role of genetic background on the COL1A2 *oim* skeletal phenotype throughout postnatal mouse development. Bone biomechanical integrity can be partitioned into the following contributing components: the amount, architecture and distribution, and bone material composition and strength [32,33]. The experimental approach we took was to examine bone biomechanical integrity of femurs from two distinct mouse strains and three genotypes at three age points. Specifically we evaluated the femoral structural integrity by determining the torsional ultimate strength T_{max}, torsional stiffness K_s, and strain energy to failure U, which are a function of both the geometry (accessed by μCT) and bone biomechanical material properties (defined by tensile strength Su and shear modulus of elasticity G). Subtle changes in either bone geometry or material properties can have a large impact on the biomechanical strength and stiffness of the skeletal component [34,35]. Bone is a composite material, which can be further subdivided into its two contributing components: the organic phase (mainly type I collagen) and the mineral phase (primarily hydroxyapatite). The combination of type I collagen and hydroxyapatite gives the bone material properties unlike either component alone [36]. Collagen content was determined using the hydroxyproline assay. Hydroxyproline, an amino acid unique to collagen, is used as an indirect measure of the amount of collagen in a tissue [28]. Since the primary collagen type in bone is type I collagen, this assay was used as a relative measure of the impact of the genetic background and the *oim* mutation on the amount of type I collagen in the bone. The hydroxyapatite crystals are normally composed of calcium, phosphate and hydroxy ions, $[3Ca_3(PO_4)_2]\bullet(OH)_2$, although several other trace minerals are present and known to impact crystal formation and alignment [14,37]. Neutron activation analysis is a unique, non-destructive method that allows

quantitation of individual trace minerals within the bone. Using these multiple levels of analyses (3 dimensional geometry, biomechanical strength and stiffness, biochemical, and mineralization), we were able to characterize both the B6-*oim* and outbred *oim* mouse lines and show that B6-*oim/oim* mice typically have a more severe clinical phenotype than do outbred *oim/oim* mice.

Inbred mouse strains have long been used to examine the contribution of genetic background to a given trait. Studies comparing the bone shape and quality of C3H/HeJ (C3) and C57BL/6J (B6) mice found several key differences in both geometry and femoral strength. C3 mice have higher femoral bone mineral density and thicker cortices compared to B6 mice, although both strains fall within the normal range of bone mineral densities for mice [19,38]. C3 mice also had a smaller cross-sectional area, but twice the bone volume as compared to B6 [20]. These geometric differences predict that C3 mice should have stronger bones, which was confirmed by biomechanical studies [20]. Consistent with this, B6 mice also have an increased osteoclast surface, but reduced osteoid surface, as compared to C3 [20], indicating that B6 animals have increased bone resorption with a reduction in the area of bone formation. This is further supported by a recent study in which a mutation was identified in the alkaline phosphatase, a marker of bone formation, gene in normal B6 animals [39].

Alterations in bone geometry contributing to bone strength throughout postnatal development have also been studied in inbred strains of mice. At E18.5 and P1, differences in bone size and shape between C3 and B6 femurs can already be seen [38,40]. By one month of age, C3 mice have a greater cortical bone width coupled with a smaller marrow cavity diameter than B6 femurs and these differences persist and become more exaggerated until one year of age [38, 40]. Additionally, by 12 weeks of age, C3 femurs have thicker trabeculi and smaller trabecular separation compared to B6 femurs [41]. These findings suggest that differences in adult bone shape and strength may be due to allelic variability that influences *in utero* bone development and that these differences persist throughout life.

The *oim* mutation arose spontaneously in an outbred B6C3Fe mouse and currently is maintained by Jackson Laboratory on this outbred genetic background. The B6C3Fe strain is an F_2 outbred of two inbred strains, C57BL/6J and C3H/HeJ. The combination of the two genetic backgrounds which have very different bone mineral densities and biomechanical strengths gives the outbred strain a great deal of variation in phenotypic severity. Each F_2 offspring will receive a unique combination of genes from each of the two genetic backgrounds. Because of the contribution of the B6 genetic background to the outbred genetic background, we predict that differences between the two strains (inbred B6 and outbred B6C3Fe) would occur due to the contribution of the C3 strain to the outbred strain, and that these differences would not be as drastic as comparisons between the two very dissimilar inbred strains, such as C57BL/6J and C3H/HeJ.

In the current study, mice of all genotypes and both genetic backgrounds exhibited an increase in body mass with age. The significant impact of the *oim/oim* mutation on somatic growth was demonstrated in mice of both genetic backgrounds as *oim/oim* mice at four months of age had similar body mass as wildtype mice of the same genetic background at one month of age. Additionally, *oim/oim* animals were able to improve their bone biomechanical strength with age. *Oim/oim* animals of both mouse strains at four months of age had similar biomechanical profiles as *oim*/+ mice of the same strain at one month of age for T_{max}, Su and U. This finding indicates that, over time, *oim/oim* mice are somewhat able to compensate for their weaker bone at both the material and femoral structural (whole bone) levels, although they are not able to reach Wt levels. Previous studies on normal [42–44] and *oim* [11,12,14] bone have focused on those changes occurring at increased age and have found substantial differences between young and old bone. McBride et al. demonstrated that the peak torque of *oim/oim* bones was

significantly reduced as compared to Wt and *oim*/+ bone at six months of age. But, at 12 months of age *oim/oim* and *oim*/+ bones had the same peak torque, though both were still greatly reduced compared to Wt [11]. This is consistent with the observation that bone from OI patients plays "catch-up" with increasing age in an attempt to compensate for the reduction in the amount and integrity of the bone [24]. The Brtl and Mov-13 mouse models of OI have also shown age-associated changes in bone integrity [25,32]. Both of these models carry mutations in the α1(I) chain and only the heterozygote animals have been evaluated. The Brtl model is a glycine to cysteine substitution in the α1(I) chain leading to an OI type IV-like phenotype [45]. The Mov-13 model is a transgenic model carrying a murine retrovirus in the first intron of the COL1A1 gene resulting in a null allele and an OI type I-like phenotype [46]. Femurs from Brtl mice had reduced maximum load compared to Wt at three months of age [25]. However, by 12 months of age, Brtl femurs were able to resist the same loads as Wt femurs [25]. This is consistent with observations that post-pubertal fracture number tends to decrease in OI patients [23]. The Mov-13 mouse model also demonstrated age-associated improvements in bone strength as well as geometry [32]. Though *oim/oim* mice represent type III OI patients, the current data are consistent with findings in mouse models of type I (Mov-13) and type IV (Brtl) OI, which both demonstrated age-associated improvements in femoral geometry and strength [25,32].

When the mineral phase of the bone was examined, several minerals were found to associate with biomechanical strength and energy to failure. Fluoride and magnesium were negatively associated with femoral bone strength and energy to failure, while sodium was positively associated. It is thought that the thinner type I collagen fibrils found in OI patients may leave more intermolecular space to be filled with mineral [34]. As the animal ages, this mineral filled space may become more pronounced than at younger ages. This is seen by age-associated increases in calcium and phosphorus in animals of all genotypes and of both genetic backgrounds.

Fluoride, known to substitute for the hydroxy group to form a less soluble fluorohydroxyapatite crystal [47], was unique from the other minerals in that it associated with bone strength in an age-dependent manner, with distinct fluoride profiles for each age group. Fluoride is known to have biphasic effects, being beneficial at low doses but detrimental at high doses [47]. Riggs et al showed that fluoride therapy in postmenopausal osteoporotic women caused thickening of the trabeculi, but induced loss of cortical bone, putting the bone at risk for fracture [48]. Consistent with these data, association of relatively high levels of fluoride in *oim/oim* tibias corresponds with weaker bones as seen by reductions in T_{max}, Su and U. This association is consistent for Wt B6 tibias, which have higher levels of fluoride and are weaker than outbred Wt tibias. *Oim*/+ tibias of both strains are intermediate to Wt and *oim/oim* in both fluoride levels and biomechanical integrity. Magnesium, thought to inhibit crystal formation by competing with calcium and blocking the active crystal growth sites [49,50], also demonstrated a negative association with bone strength and energy to failure. Fratzl et al demonstrated that *oim/oim* cortical bone has thinner and less well aligned crystals, contributing to the reduced strength of the bone [51]. As reduced magnesium is known to increase crystal size and perfection, the decrease in magnesium levels throughout postnatal development may allow the crystal size and perfection to increase along with the biomechanical integrity of the bone [52]. The role of sodium in the bone remains unclear. In conclusion, trace mineral composition, especially fluoride, magnesium and sodium, appear to play an important role in determining biomechanical femoral strength, regardless of genotype or genetic background and should be investigated further.

The main difference in collagen content, as measured by hydroxyproline content, was seen between strains and between Wt and *oim/oim* animals, regardless of strain. Outbred mice of all genotypes reached their peak hydroxyproline content at two months of age, while B6 mice

of all genotypes continued to accumulate collagen until four months of age. *Oim/oim* femurs had significantly reduced hydroxyproline levels as compared to Wt hydroxyproline levels, consistent with previous findings in which *oim/oim* animals had reduced hydroxyproline levels in bone, tendon and aorta [12,13,15]. In these animals, continued accumulation of collagen will also allow for continued accumulation of mineral. Additionally, pyridinoline crosslinks in serum were highest at two months of age, regardless of genetic background or genotype. B6 mice, as well as outbred wildtype mice, experienced a sharp reduction in the amount of pyridinoline between two and four months of age. This may be a reflection of changes in bone remodeling associated with adolescence in mice, as two and four months of age in mice correspond to puberty and post-puberty, respectively, in humans. Puberty is a time of rapid growth while bone remodeling slows dramatically during post-puberty [21]. Genotype differences in serum pyridinoline content were not seen in this study. The significance of this finding is unclear as previous studies have found both increased and decreased crosslinking in *oim/oim* animals, although crosslinking characteristics are unique to the tissue containing them [13,53,54]. The combination of age-associated accumulation of both mineral and organic phases of the bone and a decrease in bone turnover may account for the increase in biomechanical integrity of bone with age.

Over 850 OI-causing mutations in humans are known, yet understanding of genotype-phenotype relationships is still limited [17,18]. It is known that the identity of the substituting amino acid plays a role in clinical outcome as certain amino acids, such as aspartate, are more devastating than others, due to the destabilizing effects on the triple helix [18,55]. The identity of the chain harboring the mutation is also important, as each chain is proposed to have a unique distribution of lethal and non-lethal regions [56,57]. However, this does not fully explain the broad range of clinical outcomes seen in OI patients or the inter- and intrafamilial variation seen in clinical severity, suggesting that modifier genes exist, which may impact collagen gene function and, thus, affect the clinical outcome of OI-causing mutations. For example, cortical bone width contributes to the strength of the bone, but the *Col1a2* locus does not contribute to this parameter, so variability seen in the cortical bone width was due solely to the contribution of the genetic background of the animal. Therefore, therapies that target increasing the cortical bone width may improve femoral biomechanical properties independent of the *oim* mutation.

In conclusion, several age-related differences in bone structural and material properties exist in *oim/oim* animals that may allow the animals to compensate for their weaker bone material. *Oim/oim* femurs gained in their percent biomechanical strength relative to, but not reaching, Wt levels, remaining weaker than wildtype femurs regardless of strain or age. B6 femurs were also weaker than outbred femurs of like genotypes at all ages. This suggests that genetic background plays a significant role in determining the severity of the *oim* mutation. In addition, although *oim/oim* animals were able to compensate to some degree for their weaker bone material, they were not able to attain the same bone biomechanical integrity as wildtype animals with age. Taken together, these studies indicate the importance of genetic background in determining phenotypic severity, but that the presence of the *oim* mutation and the age of the animal are the primary determinants of phenotypic severity. Defining those genes that significantly contribute to the phenotypic severity of OI-causing mutations may potentially be new targets for therapies aimed at improving the bone strength and quality of life for OI patients.

ACKNOWLEDGEMENTS

We would like to acknowledge and thank Dr. Said Daibes-Figueroa and Dr. Timothy Hoffman and the Biomolecular Imaging Center, Harry S. Truman Memorial Veterans Hospital for their contributions to this project and Dr. Mark Ellersieck for his invaluable assistance with statistical analyses as well as the Leda J. Sears Trust and the Life Sciences Fellowship (SMC), the Life Science Undergraduate Research Opportunity (KMR, KLT) programs, and The Charitable and Research Foundation (DJM) for financial support.

Funding Sources: Leda J. Sears Trust Foundation (SMC, CLP); Charitable and Research Foundation (DJM); NIH Grant T32 RR07004 (CTW); DOE Grant FG07-03ID14531 (SMC, CEB, JSM, CLP); USDA CSREES NRI Grant 2006-35616-16697 (JFT)

REFERENCES

1. Byers, PH. Connective Tissue and Its Heritable Disorders. New York: Wiley-Liss; 1993. Osteogenesis Imperfecta.
2. Jimenez SA, Bashey RI, Benditt M, Yankowski R. Identification of collagen alpha1(I) trimer in embryonic chick tendons and calvaria. Biochem Biophys Res Commun 1977;78:1354–1361. [PubMed: 562664]
3. Scriver, CR. The Metabolic basis of inherited disease. New York: McGraw-Hill; 1989.
4. Moro L, Smith BD. Identification of collagen alpha1(I) trimer and normal type I collagen in a polyoma virus-induced mouse tumor. Arch Biochem Biophys 1977;182:33–41. [PubMed: 196556]
5. Uitto J. Collagen polymorphism: isolation and partial characterization of alpha 1(I)-trimer molecules in normal human skin. Arch Biochem Biophys 1979;192:371–379. [PubMed: 434832]
6. Rupard JH, Dimari SJ, Damjanov I, Haralson MA. Synthesis of type I homotrimer collagen molecules by cultured human lung adenocarcinoma cells. Am J Pathol 1988;133:316–326. [PubMed: 3189509]
7. Haralson MA, Jacobson HR, Hoover RL. Collagen polymorphism in cultured rat kidney mesangial cells. Lab Invest 1987;57:513–523. [PubMed: 3682763]
8. Cohen, IK.; Diegelmann, RF.; Lindblad, WJ. Wound healing : biochemical & clinical aspects. Philadelphia: W.B. Saunders Co.; 1992.
9. Sillence DO, Senn A, Danks DM. Genetic heterogeneity in osteogenesis imperfecta. J Med Genet 1979;16:101–116. [PubMed: 458828]
10. Chipman SD, Sweet HO, McBride DJ Jr, Davisson MT, Marks SC Jr, Shuldiner AR, Wenstrup RJ, Rowe DW, Shapiro JR. Defective pro alpha 2(I) collagen synthesis in a recessive mutation in mice: a model of human osteogenesis imperfecta. Proc Natl Acad Sci U S A 1993;90:1701–1705. [PubMed: 8446583]
11. McBride DJ Jr, Shapiro JR, Dunn MG. Bone geometry and strength measurements in aging mice with the oim mutation. Calcif Tissue Int 1998;62:172–176. [PubMed: 9437052]
12. Camacho NP, Hou L, Toledano TR, Ilg WA, Brayton CF, Raggio CL, Root L, Boskey AL. The material basis for reduced mechanical properties in oim mice bones. J Bone Miner Res 1999;14:264–272. [PubMed: 9933481]
13. Pfeiffer BJ, Franklin CL, Hsieh FH, Bank RA, Phillips CL. Alpha 2(I) collagen deficient oim mice have altered biomechanical integrity, collagen content, and collagen crosslinking of their thoracic aorta. Matrix Biol 2005;24:451–458. [PubMed: 16095890]
14. Phillips CL, Bradley DA, Schlotzhauer CL, Bergfeld M, Libreros-Minotta C, Gawenis LR, Morris JS, Clarke LL, Hillman LS. Oim mice exhibit altered femur and incisor mineral composition and decreased bone mineral density. Bone 2000;27:219–226. [PubMed: 10913914]
15. McBride DJ Jr, Choe V, Shapiro JR, Brodsky B. Altered collagen structure in mouse tail tendon lacking the alpha 2(I) chain. J Mol Biol 1997;270:275–284. [PubMed: 9236128]
16. Weis SM, Emery JL, Becker KD, McBride DJ Jr, Omens JH, McCulloch AD. Myocardial mechanics and collagen structure in the osteogenesis imperfecta murine (oim). Circ Res 2000;87:663–669. [PubMed: 11029401]
17. Dalgleish R. The Human Collagen Mutation Database 1998. Nucleic Acids Res 1998;26:253–255. [PubMed: 9399846]
18. Marini JC, Forlino A, Cabral WA, Barnes AM, San Antonio JD, Milgrom S, Hyland JC, Korkko J, Prockop DJ, De Paepe A, Coucke P, Symoens S, Glorieux FH, Roughley PJ, Lund AM, Kuurila-Svahn K, Hartikka H, Cohn DH, Krakow D, Mottes M, Schwarze U, Chen D, Yang K, Kuslich C, Troendle J, Dalgleish R, Byers PH. Consortium for osteogenesis imperfecta mutations in the helical domain of type I collagen: regions rich in lethal mutations align with collagen binding sites for integrins and proteoglycans. Hum Mutat 2007;28:209–221. [PubMed: 17078022]
19. Beamer WG, Donahue LR, Rosen CJ, Baylink DJ. Genetic variability in adult bone density among inbred strains of mice. Bone 1996;18:397–403. [PubMed: 8739896]

20. Akhter MP, Iwaniec UT, Covey MA, Cullen DM, Kimmel DB, Recker RR. Genetic variations in bone density, histomorphometry, and strength in mice. Calcif Tissue Int 2000;67:337–344. [PubMed: 11000349]
21. Specker BL, Schoenau E. Quantitative bone analysis in children: current methods and recommendations. J Pediatr 2005;146:726–731. [PubMed: 15973307]
22. Skerry TM. One mechanostat or many? Modifications of the site-specific response of bone to mechanical loading by nature and nurture. J Musculoskelet Neuronal Interact 2006;6:122–127. [PubMed: 16849820]
23. Paterson CR, McAllion S, Stellman JL. Osteogenesis imperfecta after the menopause. N Engl J Med 1984;310:1694–1696. [PubMed: 6727948]
24. Ramser JR, Villanueva AR, Pirok D, Frost HM. Tetracycline-based measurement of bone dynamics in 3 women with osteogenesis imperfecta. Clin Orthop Relat Res 1966;49:151–162. [PubMed: 5962613]
25. Kozloff KM, Carden A, Bergwitz C, Forlino A, Uveges TE, Morris MD, Marini JC, Goldstein SA. Brittle IV mouse model for osteogenesis imperfecta IV demonstrates postpubertal adaptations to improve whole bone strength. J Bone Miner Res 2004;19:614–622. [PubMed: 15005849]
26. Roarck, RJ.; Young, WC. Formulas for Stress and Strain. McGraw-Hill: Formulas for Stress and Strain; 1975.
27. Buff CE, Carleton SM, McBride DJ Jr, Phillips CL, Morris JS. Multi-element analysis of bone from the osteogenesis imperfecta model (oim) mouse using thermal and fast neutron activation analysis. Accepted for Publication: Journal of Radioanalytical and Nuclear Chemistry. 2006
28. Woessner JF Jr. The determination of hydroxyproline in tissue and protein samples containing small proportions of this imino acid. Arch Biochem Biophys 1961;93:440–447. [PubMed: 13786180]
29. Stegemann H, Stalder K. Determination of hydroxyproline. Clin Chim Acta 1967;18:267–273. [PubMed: 4864804]
30. Searle, SR. Linear Models. New York: John Wiley and Sons; 1971.
31. Conover WJ, Iman RL. Analysis of covariance using the rank transformation. Biometrics 1982;38:715–724. [PubMed: 7171697]
32. Bonadio J, Jepsen KJ, Mansoura MK, Jaenisch R, Kuhn JL, Goldstein SA. A murine skeletal adaptation that significantly increases cortical bone mechanical properties. Implications for human skeletal fragility. J Clin Invest 1993;92:1697–1705. [PubMed: 8408623]
33. van der Meulen MC, Jepsen KJ, Mikic B. Understanding bone strength: size isn't everything. Bone 2001;29:101–104. [PubMed: 11502469]
34. Rauch F. Material matters: a mechanostat-based perspective on bone development in osteogenesis imperfecta and hypophosphatemic rickets. J Musculoskelet Neuronal Interact 2006;6:142–146. [PubMed: 16849823]
35. Turner CH. Bone strength: current concepts. Ann N Y Acad Sci 2006;1068:429–446. [PubMed: 16831941]
36. Burr DB. The contribution of the organic matrix to bone's material properties. Bone 2002;31:8–11. [PubMed: 12110405]
37. Baron, R. Anatomy and ultrastructure of bone. Primer on the Metabolic Bone Diseases and Disorders of Mineral Metabolism. Philadelphia: Lippincott Williams and Wilkins; 1999.
38. Richman C, Kutilek S, Miyakoshi N, Srivastava AK, Beamer WG, Donahue LR, Rosen CJ, Wergedal JE, Baylink DJ, Mohan S. Postnatal and pubertal skeletal changes contribute predominantly to the differences in peak bone density between C3H/HeJ and C57BL/6J mice. J Bone Miner Res 2001;16:386–397. [PubMed: 11204439]
39. Klein, RF.; Carlos, AS.; Kansagor, JN.; Olson, DA.; Wagoner, WJ.; Larson, EA.; Dinulescu, DC.; Munsey, TG.; Vanek, C.; Madison, DL.; Landblad, JR.; Belknap, JK.; Orwoll, ES. Identification of Akp2 as a gene that tregulates peak bone mass in mice. American Society of Bone and Mineral Research, 27th Annual Meeting; September, 2005; Nashville, TN. 2005.
40. Turner CH, Sun Q, Schriefer J, Pitner N, Price R, Bouxsein ML, Rosen CJ, Donahue LR, Schultz KL, Beamer WG. Congenic mice reveal sex-specific genetic regulation of femoral structure and function. Calcif Tissue Int 2003;73:297–303. [PubMed: 14667144]

41. Linkhart TA, Linkhart SG, Kodama Y, Farley JR, Dimai HP, Wright KR, Wergedal JE, Sheng M, Beamer WG, Donahue LR, Rosen CJ, Baylink DJ. Osteoclast formation in bone marrow cultures from two inbred strains of mice with different bone densities. J Bone Miner Res 1999;14:39–46. [PubMed: 9893064]
42. Vashishth D. Age-dependent biomechanical modifications in bone. Crit Rev Eukaryot Gene Expr 2005;15:343–358. [PubMed: 16472064]
43. Rosen, CJ.; Kiel, DP. Primer on the Metabolic Bone Diseases and Disorders of Mineral Metabolism. Philadelphia: Lippincott Williams and Wilkins; 1999. The aging skeleton.
44. Kloss FR, Gassner R. Bone and aging: effects on the maxillofacial skeleton. Exp Gerontol 2006;41:123–129. [PubMed: 16412598]
45. Forlino A, Porter FD, Lee EJ, Westphal H, Marini JC. Use of the Cre/lox recombination system to develop a non-lethal knock-in murine model for osteogenesis imperfecta with an alpha1(I) G349C substitution. Variability in phenotype in BrtlIV mice. J Biol Chem 1999;274:37923–37931. [PubMed: 10608859]
46. Bonadio J, Saunders TL, Tsai E, Goldstein SA, Morris-Wiman J, Brinkley L, Dolan DF, Altschuler RA, Hawkins JE Jr, Bateman JF, et al. Transgenic mouse model of the mild dominant form of osteogenesis imperfecta. Proc Natl Acad Sci U S A 1990;87:7145–7149. [PubMed: 2402497]
47. Cheng P-T, Bader SM, Grynpas MD. Biphasic sodium fluoride effects on bone and bone mineral: a review. Cells and Materials 1995;5:271–282.
48. Riggs BL, O'Fallon WM, Lane A, Hodgson SF, Wahner HW, Muhs J, Chao E, Melton LJ 3rd. Clinical trial of fluoride therapy in postmenopausal osteoporotic women: extended observations and additional analysis. J Bone Miner Res 1994;9:265–275. [PubMed: 8140940]
49. Bigi A, Foresti E, Gregorini R, Ripamonti A, Roveri N, Shah JS. The role of magnesium on the structure of biological apatites. Calcif Tissue Int 1992;50:439–444. [PubMed: 1596779]
50. Steinfort J, Driessens FC, Heijligers HJ, Beertsen W. The distribution of magnesium in developing rat incisor dentin. J Dent Res 1991;70:187–191. [PubMed: 1999557]
51. Fratzl P, Paris O, Klaushofer K, Landis WJ. Bone mineralization in an osteogenesis imperfecta mouse model studied by small-angle x-ray scattering. Journal of Clinical Investigation 1996;97:396–402. [PubMed: 8567960]
52. Boskey AL, Rimnac CM, Bansal M, Federman M, Lian J, Boyan BD. Effect of short-term hypomagnesemia on the chemical and mechanical properties of rat bone. J Orthop Res 1992;10:774–783. [PubMed: 1403290]
53. Miles CA, Sims TJ, Camacho NP, Bailey AJ. The role of the alpha2 chain in the stabilization of the collagen type I heterotrimer: a study of the type I homotrimer in oim mouse tissues. J Mol Biol 2002;321:797–805. [PubMed: 12206762]
54. Paschalis EP, Shane E, Lyritis G, Skarantavos G, Mendelsohn R, Boskey AL. Bone fragility and collagen cross-links. J Bone Miner Res 2004;19:2000–2004. [PubMed: 15537443]
55. Persikov AV, Pillitteri RJ, Amin P, Schwarze U, Byers PH, Brodsky B. Stability related bias in residues replacing glycines within the collagen triple helix (Gly-Xaa-Yaa) in inherited connective tissue disorders. Hum Mutat 2004;24:330–337. [PubMed: 15365990]
56. Marini JC, Lewis MB, Wang Q, Chen KJ, Orrison BM. Serine for glycine substitutions in type I collagen in two cases of type IV osteogenesis imperfecta (OI). Additional evidence for a regional model of OI pathophysiology. J Biol Chem 1993;268:2667–2673. [PubMed: 8094076]
57. Wang Q, Orrison BM, Marini JC. Two additional cases of osteogenesis imperfecta with substitutions for glycine in the alpha 2(I) collagen chain. A regional model relating mutation location with phenotype. J Biol Chem 1993;268:25162–25167. [PubMed: 7693712]

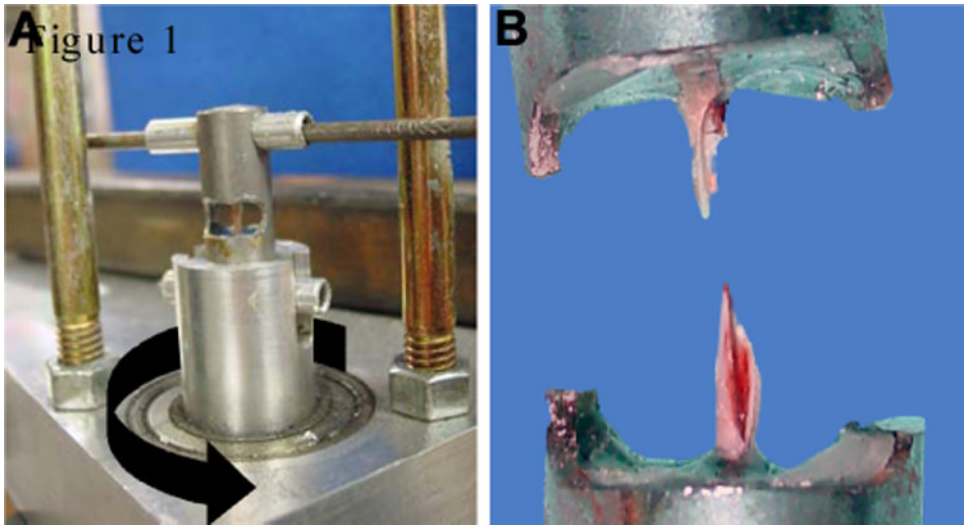

Figure 1.

Femoral torsional loading to failure. A) The testing fixture restrains the top end of the femur holder from axial rotation while the bottom is axially rotated (indicated by *black* arrow) at a constant rate of 0.75 rad/sec by a cable wrapped around the ball bearing supported shaft and pulled by the 5 kg load cell attached to the test machine's crosshead. Struts (indicated by *white* arrows) are cut prior to rotation. B) A typical post-test spiral fracture.

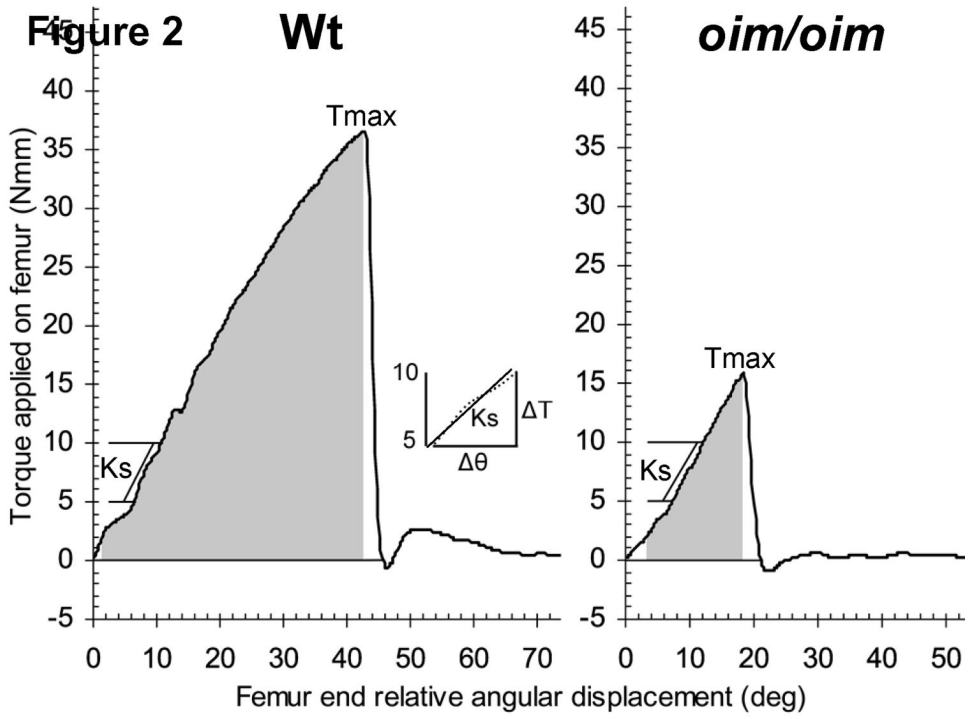

Figure 2.

Representative graphs showing femur torque versus angular displacement for outbred Wt and *oim/oim* femurs at four months of age. Torsional ultimate strength T_{max} is the maximum applied torque required to fracture the bone. Energy to failure U (shaded area) is the amount of strain energy the bone can absorb prior to fracture. Insert illustrates a least-squares fit line to data from five to ten Nmm with the torsional stiffness Ks derived from the slope of this line.

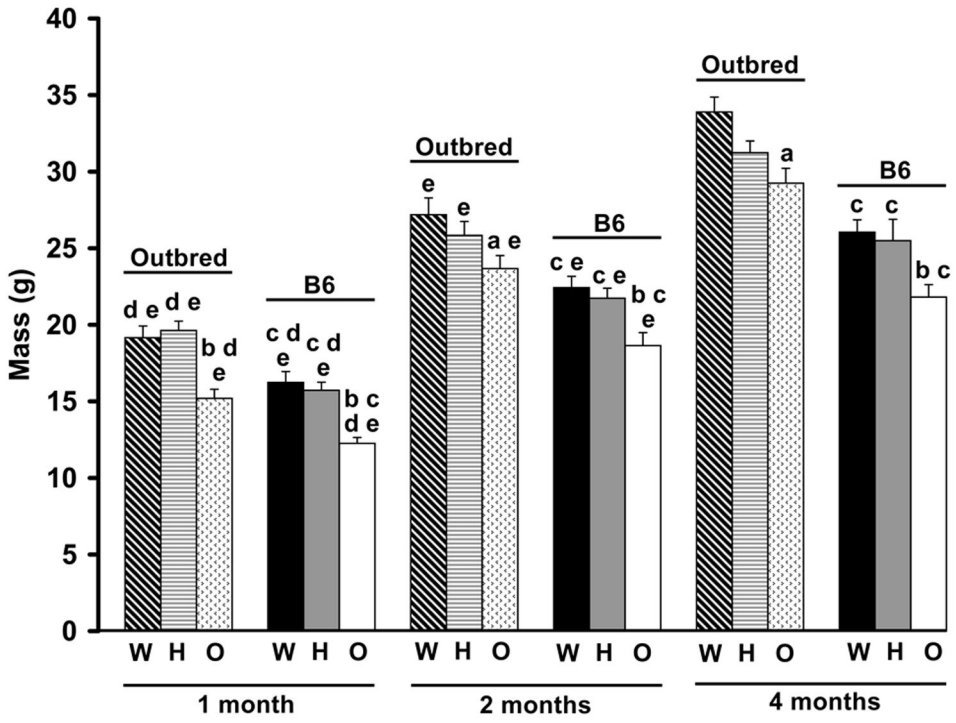

Figure 3.

Total body mass of B6 and outbred Wt, *oim*/+ and *oim/oim* mice at 1, 2 and 4 months of age. *Oim/oim* mice had reduced body mass compared to Wt and *oim*/+ at all ages, regardless of strain. B6 mice also had reduced body mass compared to age and genotype matched outbred animals. [a]$p \leq 0.05$ as compared to Wt animals of the same strain and age; [b]$p \leq 0.05$ as compared to Wt and *oim*/+ animals of the same strain and age; [c]$p \leq 0.05$ as compared to outbred animals of the same genotype and age; [d]$p \leq 0.05$ as compared to 2 month animals of the same genotype and strain; [e]$p \leq 0.05$ as compared to 4 month animals of the same genotype and strain. [per age class: Wt, n=12–21; *oim*/+, n=11–36; *oim/oim*, n=7–19]

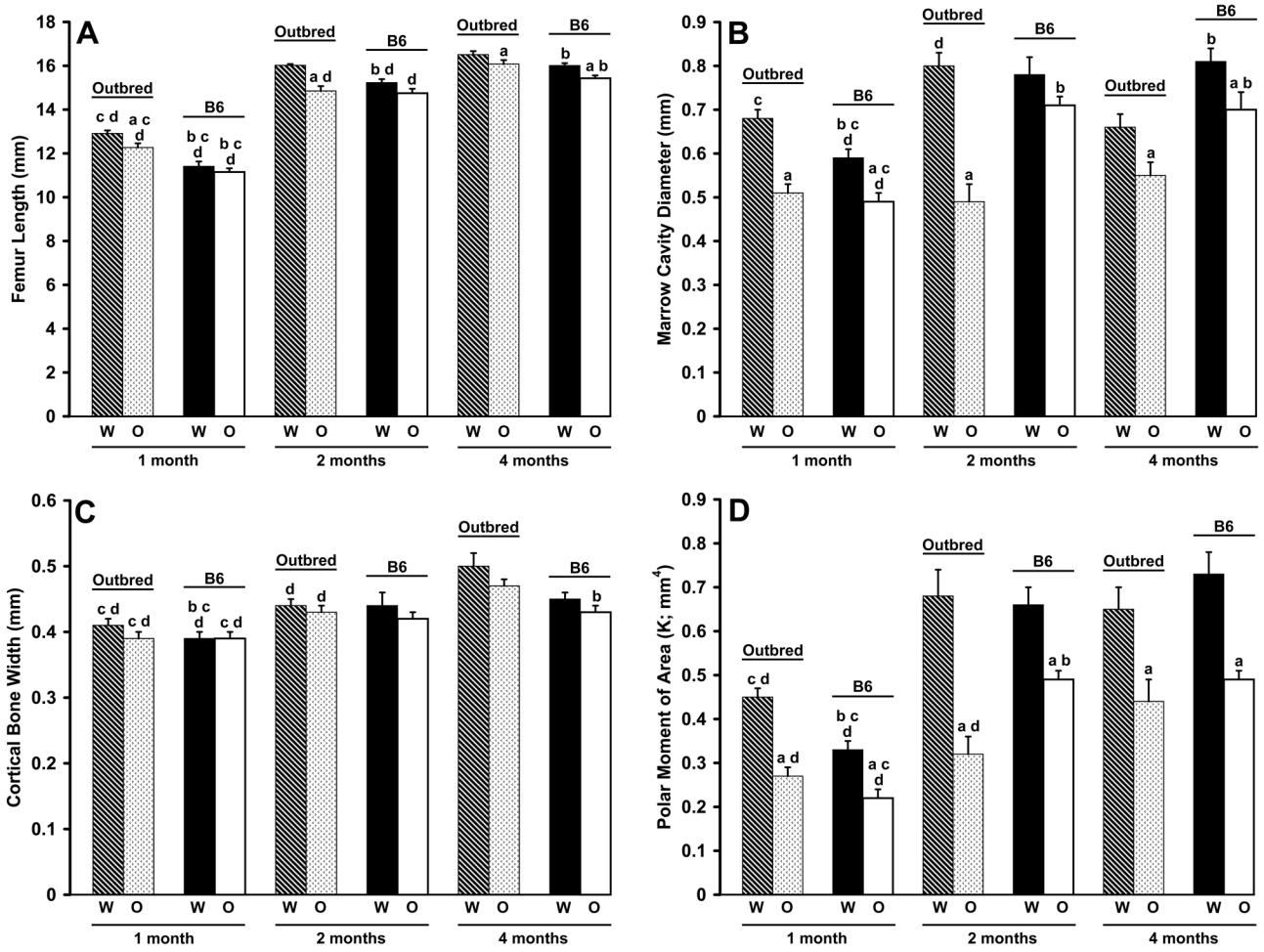

Figure 4.

Femoral geometry of B6 and outbred Wt, *oim*/+ and *oim/oim* mice at 1, 2 and 4 months of age. A) Femur length exhibited strain differences in Wt (all ages) and *oim/oim* femurs (1 and 4 months). Outbred Wt femurs were longer than *oim/oim* femurs (all ages); B6 Wt femurs were longer than *oim/oim* femurs (4 months). B) Marrow cavity diameter (MCD) showed strain differences in Wt animals (1 and 4 months) and in *oim/oim* animals (2 and 4 months). Wt femurs of both strains had larger MCDs than *oim/oim* femurs (1 and 4 months); outbred Wt femurs were also larger at 2 months. C) Cortical bone width (CBW) had strain differences in Wt femurs (1 month) and in *oim/oim* femurs (4 months). D) Polar moment of area (K) showed strain differences in Wt femurs (1 month) and in *oim/oim* femurs (2 months). Wt femurs had a larger K than *oim/oim* femurs in both strains at all ages. $^{a}p\leq0.05$ as compared to Wt femurs of the same strain and age; $^{b}p\leq0.05$ as compared to outbred femurs of the same genotype and age; $^{c}p\leq0.05$ as compared to 2 month femurs of the same genotype and strain; $^{d}p\leq0.05$ as compared to 4 month femurs of the same genotype and strain. [per age class: Wt, n=8–18; *oim*/+, n=8–15; *oim/oim*, n=8–14]

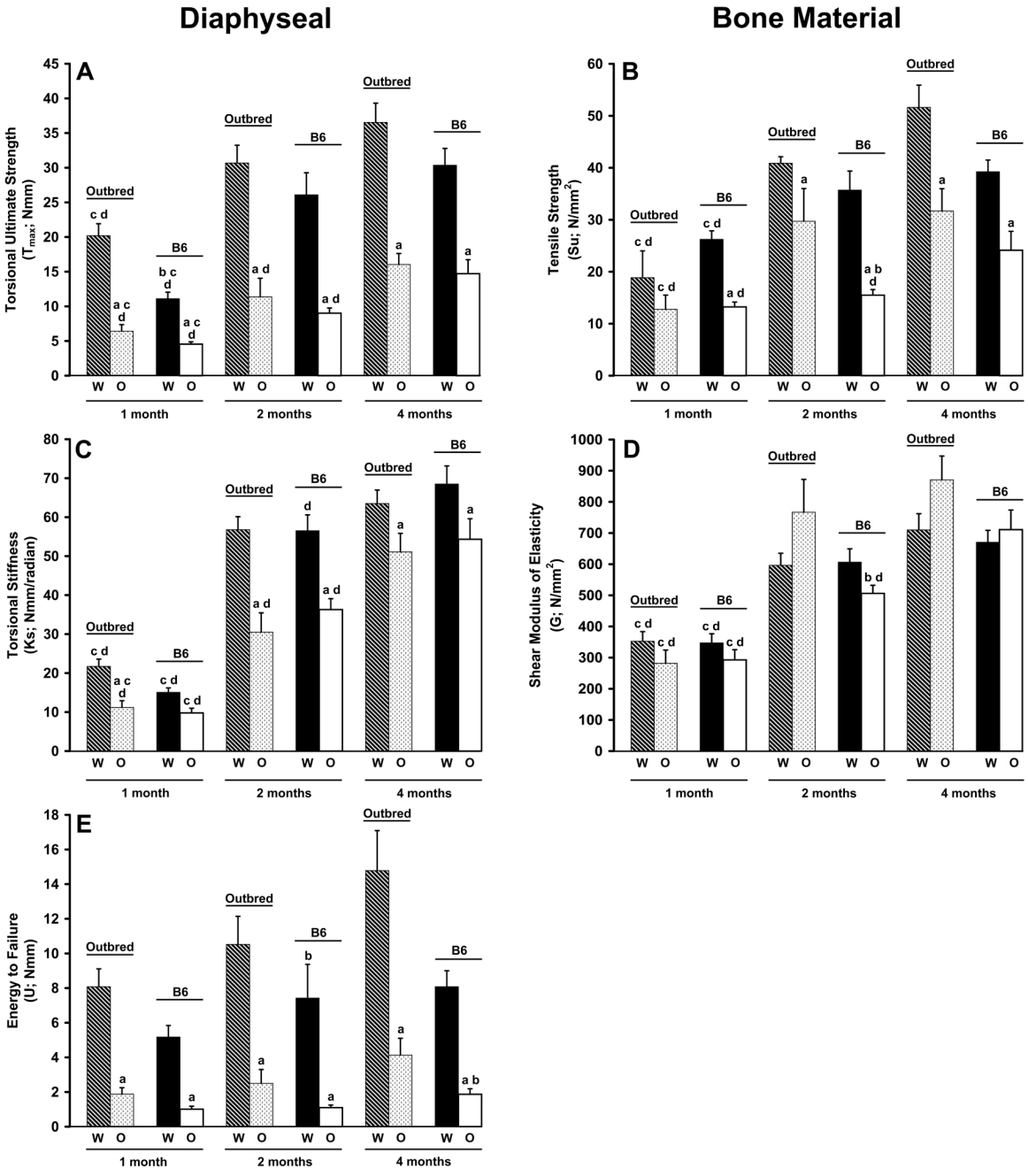

Figure 5.

Femoral diaphyseal structural and cortical bone material biomechanical properties determined by torsional loading to failure. Diaphyseal A) torsional loading to failure T_{max} and cortical bone B) tensile strength Su improve with age in both strains and genotypes, although *oim/oim* remain weaker than Wt at all ages. Diaphyseal E) energy to failure U was significantly reduced in *oim/oim* femurs as compared to Wt in both strains and at all ages. Diaphyseal C) torsional stiffness K and cortical bone D) shear modulus of elasticity G increased in both strains and genotypes with age. [a]$p \leq 0.05$ as compared to Wt femurs of the same strain and age; [b]$p \leq 0.05$ as compared to outbred femurs of the same genotype and age; [c]$p \leq 0.05$ as compared to 2 month

femurs of the same genotype and strain; [d]$p \leq 0.05$ as compared to 4 month femurs of the same genotype and strain. [per age class: Wt, n=8–12; *oim*/+, n=6–12; *oim/oim*, n=6–12]

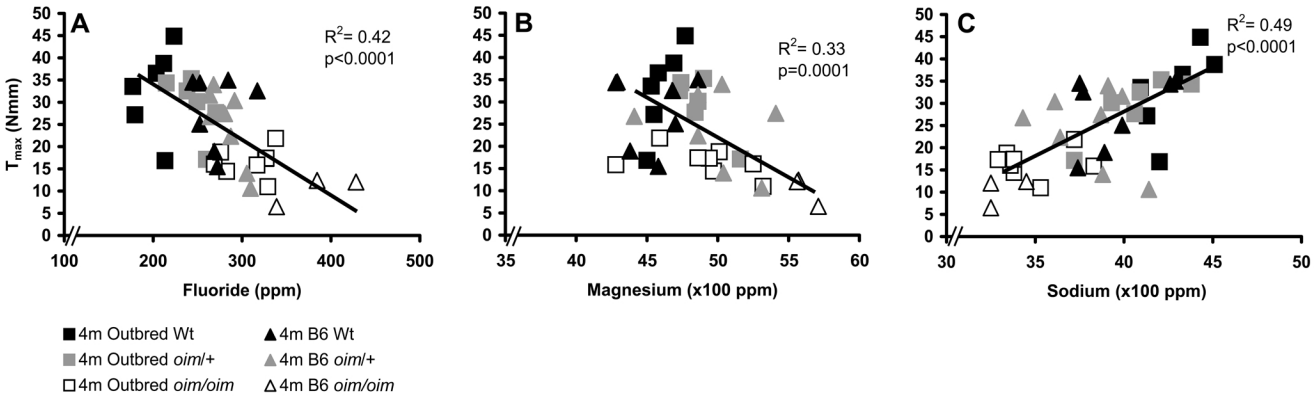

Figure 6.

Association of fluoride, magnesium and sodium levels with femoral strength. A) Fluoride and B) magnesium are negatively associated, while C) sodium is positively associated with femoral diaphyseal ultimate strength T_{max} in all genotypes. Bone material tensile strength Su and energy to failure U also associate with these minerals in a manner similar to T_{max} (data not shown), while no association was found between mineral levels and stiffness properties diaphyseal Ks or material G (data not shown). [per age class: n=7–8 of each strain/genotype]

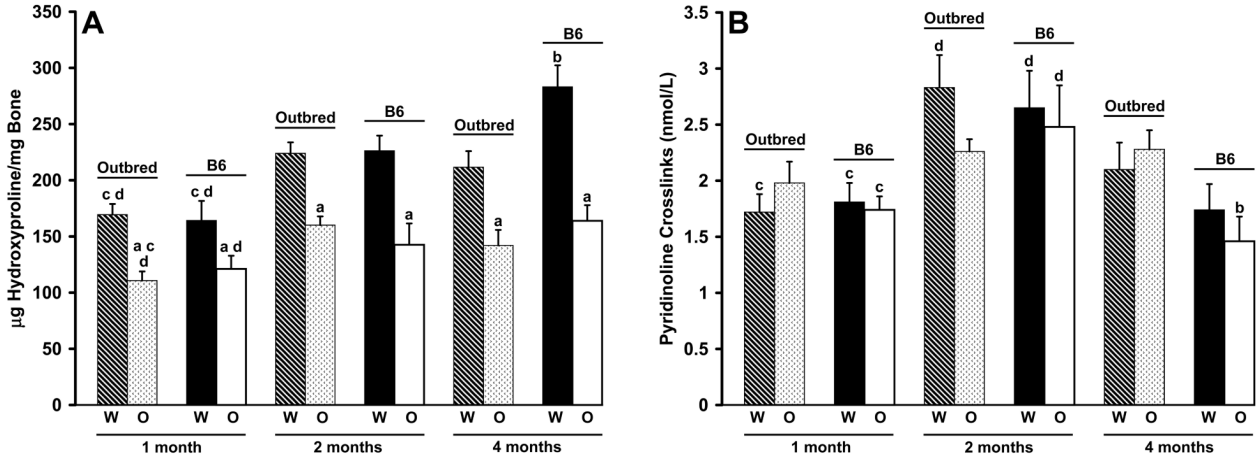

Figure 7.

Femoral hydroxyproline content and serum pyridinoline content. A) B6 animals demonstrate age-related increases in hydroxyproline content at all ages while outbred animals only show an increase at two months of age with a decrease at four months of age. Strain differences were seen in Wt animals (4 months). Wt femurs of both strains had increased hydroxyproline content compared to *oim/oim* femurs at all ages. [per age class: Wt, n=7–13; *oim*/+, n=8–10; *oim/oim*, n=7–13] B) Pyridinoline content of serum at one, two and four months of age. Genotype differences were not seen at any age in either strain. Pyridinoline crosslinks were highest at two months of age in both strains and genotypes. [a]$p \leq 0.05$ as compared to Wt femurs of the same strain and age; [b]$p \leq 0.05$ as compared to outbred femurs of the same genotype and age; [c]$p \leq 0.05$ as compared to 2 month femurs of the same genotype and strain; [d]$p \leq 0.05$ as compared to 4 month femurs of the same genotype and strain. [per age class Wt, n=7–9; *oim*/+, n=7–9; *oim/oim*, n=5–8]

Table 1

Instrumental Neutron Activation Analysis Parameters

Ion	Nuclear Reaction	Photopeak (keV)	Irradiation Time[a]	Irradiation Time[b]	Decay Time	Count Time	Count Position
F	$F^{19}(n,\gamma)F^{20}$	1633	7 sec	15 sec	15 sec	30 sec	Face
P	$P^{31}(n,\alpha)Al^{28}$	1779	15 sec	15 sec	1 min	3 min	Face
Na	$Na^{23}(n,\gamma)Na^{24}$	1368	7 sec	15 sec	1 min	10 min	1 spin[d]
Mg	$Mg^{26}(n,\gamma)Mg^{27}$	844, 1014	7 sec	15 sec	1 min	10 min	1 spin
Ca	$Ca^{48}(n,\gamma)Ca^{49}$	3085	7 sec	15 sec	1 min	10 min	1 spin
K	$K^{41}(n,\gamma)K^{42}$	1524	95 sec	360 sec	EOI[c]	30 min	1[e]
Zn	$Zn^{68}(n,\gamma)Zn^{69m}$	438	95 sec	360 sec	EOI[c]	30 min	1[e]

[a] Irradiation time for tibiae from two and four month old animals.

[b] Irradiation time for tibiae from one month old animals.

[c] EOI: End of Irradiation Time is the specific time the sample exited the reactor. All samples and standards were decay corrected back to this time.

[d] Count position was in a rotating position 2.5 cm from the detector face.

[e] Count position was in a stationary position 2.5 cm from the detector face.

Table 2

Percent Variation Due to *oim* Mutation and Genetic Background

	Outbred		B6	
Geometry	*oim* Mutation	Genetic Background	*oim* Mutation	Genetic Background
Body Mass	36%	64%	45%	55%
Femur Length	27%	73%	11%	89%
Marrow Cavity Diameter	52%	48%	24%	76%
Cortical Bone Width	11%	89%	6%	94%
Polar Moment of Area	55%	45%	32%	68%
Biomechanics	*oim* Mutation	Genetic Background	*oim* Mutation	Genetic Background
T_{max}	67%	33%	52%	48%
Su	36%	64%	56%	44%
Ks	28%	72%	9%	91%
G	<5%	>95%	<5%	>95%
U	52%	48%	54%	46%
Collagen and Mineral; Bone Turnover	*oim* Mutation	Genetic Background	*oim* Mutation	Genetic Background
F, Mg and Na Content	41–56%[a]	44–59%[a]	69–71%[a]	29–31%[a]
Hydroxyproline	37%	63%	37%	63%
Pyridinoline Crosslinks	<5%	>95%	<5%	>95%

[a] Exact percentage is mineral specific.

Table 3

Mineral Composition of Tibiae from 1-, 2- and 4- month old Outbred and B6 Wt, *oim*/+ and *oim/oim* Mice

Mineral (ppm)	Outbred			B6		
	Wt	***oim*/+**	***oim/oim***	**Wt**	***oim*/+**	***oim/oim***
			1 month			
F	101.7±6.8^{de}	109.3±6.8^{de}	118.2±10.6^{de}	124.1±14.8^{cde}	130.7±14.3^{de}	186.6±10.5^{abcde}
P (x1000)	111.5±0.90^{de}	115.9±1.2^{ade}	114.2±3.0^{ade}	108.4±0.95^{e}	113.3±1.1^{ae}	118.7±1.3^{abde}
Na (x100)	30.6±0.85^{de}	29.6±0.88^{de}	29.3±1.31^{de}	23.6±0.78^{cde}	24.0±2.2^{cde}	16.2±0.64^{bcde}
Mg (x100)	50.6±0.84^{de}	52.5±0.68^{de}	54.0±0.83^{ae}	50.2±0.75^{e}	53.7±0.80^{ae}	56.0±0.89^{ab}
Ca (x1000)	238.9±2.4^{e}	245.0±3.1^{e}	246.1±4.4^{e}	233.0±2.3^{e}	243.5±1.8^{ae}	211.9±3.3^{ae}
Ca/P Ratio	2.14±0.01^{e}	2.11±0.01^{e}	2.16±0.02^{de}	2.15±0.01^{de}	2.15±0.02^{d}	2.06±0.02^{abcd}
K	215.4±11.1^{e}	315.2±58.5^{ae}	472.0±59.1^{abe}	160.1±43.7^{de}	170.8±20.5^{de}	82.6±15.3^{cde}
Zn	152.7±17.6^{d}	179.1±29.7^{e}	274.0±45.3^{ab}	134.3±15.5^{e}	188.7±22.6	223.5±26.9^{ad}
			2 months			
F	134.5±6.9^{e}	163.0±5.7^{ae}	254.3±31.6^{abe}	232.7±13.1^{c}	220.4±9.0^{ce}	375.2±16.5^{abc}
P (x1000)	116.4±0.71^{e}	119.9±0.49^{ae}	121.6±1.6^{ae}	112.5±1.3^{e}	115.7±1.5^{ce}	123.7±0.93^{abe}
Na (x100)	39.5±0.58^{e}	40.7±0.47	34.9±0.88^{ab}	38.6±0.58	34.7±0.89^{ace}	29.3±0.68^{abce}
Mg (x100)	46.8±0.45	48.9±0.54	54.4±1.64^{abe}	49.2±0.70^{ce}	51.6±0.63^{ac}	54.4±0.57^{ab}
Ca (x1000)	245.1±1.4^{e}	251.3±1.1^{ae}	252.0±2.6^{ae}	233.7±2.4^{ce}	238.9±2.9^{ce}	246.9±1.1^{abe}
Ca/P Ratio	2.11±0.01	2.10±0.01	2.07±0.01	2.08±0.03	2.06±0.01^{e}	2.0±0.01^{abce}
K	224.6±31.7^{e}	384.8±41.2^{a}	420.6±65.4^{a}	366.8±39.6^{c}	336.4±54.9	241.5±33.8^{ac}
Zn	241.2±20.6	205.2±28.1	335.1±28.2^{ab}	195.4±24.3	185.3±23	296.3±36.4^{ab}
			4 months			
F	200.1±6.4	237.9±8.1^{a}	308.1±9.8^{ab}	262.9±11.0^{c}	283.7±6.4^{c}	402.5±17.1^{abc}
P (x1000)	126.4±1.0	130.1±0.69	131.2±1.3^{a}	123.4±2.3	123.9±2.5^{c}	129.5±1.1^{ab}
Na (x100)	43.0±0.54	40.4±0.78^{a}	34.8±0.70^{ab}	39.7±0.80^{c}	38.1±0.82^{c}	32.8±0.68^{ab}
Mg (x100)	46.3±0.36	48.2±0.55	50.3±0.87^{a}	45.5±0.74	49.7±1.09^{a}	54.4±0.54^{abc}
Ca (x1000)	263.7±1.2	269.3±0.7	268.8±1.4	253.9±3.7^{c}	261.4±5.6^{c}	268.7±1.1^{ab}

Mineral (ppm)	Outbred			B6		
	Wt	***oim*/+**	***oim/oim***	**Wt**	***oim*/+**	***oim/oim***
Ca/P Ratio	2.09±0.02	2.07±0.01	2.05±0.01	2.06±0.04	2.11±0.02	2.08±0.01[c]
K	356.2±39.5	432.9±55.9	295.9±40.5[b]	333.9±55.5	286.2±20.0[c]	242.4±28.9
Zn	190.0±22.1	259.7±16.2[a]	311.3±26.8[a]	208.5±13.9	228.9±18.3	251.8±31.9

[a] p<0.05 compared to Wt of same strain and age

[b] p<0.05 compared to *oim*/+ of same strain and age

[c] p<0.05 compared to outbred animals of same genotype and age

[d] p<0.05 compared to 2 month animals of same genotype and strain

[e] p<0.05 compared to 4 month animals of same genotype and strain

Table 4

Relationship Between Bone Biomechanics and Bone Mineral Composition

	T_{max}			Su			U		
Mineral	**Intercept**	**Slope**	**R^2**	**Intercept**	**Slope**	**R^2**	**Intercept**	**Slope**	**R^2**
F	57.3	−0.12[b]	0.42	79.5	−0.16[b]	0.30	21.0	−0.05[b]	0.37
P	80.7	−0.0004	0.06	35.7	0.000004	0	5.6	0.000008	0
Na	−47.6	0.019[b]	0.49	−55.5	0.024[b]	0.32	−19.8	0.0069[b]	0.31
Mg	101.1	−0.016[b]	0.33	110.3	−0.015[a]	0.13	34.7	−0.0058[a]	0.21
Ca	92.0	−0.0026	0.073	72.1	−0.00014	0.0084	21.3	−0.00006	0.016
Ca/P Ratio	21.8	1.3	0	105.6	−33.4	0.018	34.8	−13.6	0.034
K	18.8	0.02	0.55	28.9	0.02	0.037	4.03	0.008	0.055
Zn	37.5	−0.05[a]	0.16	57.4	−0.09[a]	0.17	11.6	−0.02[a]	0.11

[a] $p<0.05$

[b] $p<0.001$ for significant interactions between mineral and biomechanical parameter independent of genotype, strain or age.